DESIGN AND SIMULATION OF ELECTROOSMOTIC DRIVEN FLOW IN CROSS CHANNELS

Oana Tatiana NEDELCU[1], Raluca MULLER[2], Hans G. KERKHOFF[3], Robert W. BARBER[4]

În această lucrare sunt prezentate rezultate de proiectare şi simulare ale unui sistem micro-electro-fluidic (MEF). Sistemul consta într-o rețea de microcanale în care curgerea fluidului este controlată prin efect electroosmotic. Pentru caracterizarea dispozitivului fluidic de tip "Field Effect Transistor" (FlowFET) au fost efectuate analize de simulare pentru cazul fără defecte de fabricație. Dispozitivul FlowFET funcționează prin aplicarea unei tensiuni pe un electrod situat pe o suprafață a canalului, față de care este separat printr-un strat izolator. În acest mod se poate modifica valoarea potențialului ζ în zona din vecinătatea electrodului. Variația potentialului ζ poate fi utilizata pentru a controla mărimea şi directia vitezei fluidului în rețeaua de microcanale.

A micro-electronic fluidic (MEF) system was designed and simulated. The system consists in cross-channels where the fluid flow is controlled by electroosmotic effect. Electroosmotic simulations were performed to characterize the fluidic Field Effect Transistor (FlowFET) device under fault-free conditions. The FlowFET operates by applying a voltage field from a gate electrode in the insulated side wall of a microchannel to modulate the ζ-potential at the shear plane. The change in ζ-potential can be used to control both the magnitude and direction of the electroosmotic flow in the microchannel array.

Keywords: microsystem simulation, electroosmotic flow, FlowFET systems

1. Introduction

The miniaturization of fluidic systems yields many functionalities and economical benefits, particularly for biomedical and chemical application, as reducing the fluid amount and analyses costs, low energy and reagent consumption, rapid analysis time and a high level of automation [1,2]. In

[1] National Institute for Research and Development in Microtechnology, Bucharest, Romania, Oana.Nedelcu@imt.ro
[2] MESA+ Research Institute for Nanotechnology, Testable Design and Testing of Nanosystems Group, Enschede, The Netherlands
[3] MESA+ Research Institute for Nanotechnology, Testable Design and Testing of Nanosystems Group, Enschede, The Netherlands
[4] Centre for Microfluidics and Microsystems Modelling, CCLRC Daresbury Laboratory, Warrington, Cheshire, UK

advanced application, electronic is merged with the fluidic modules [3], to perform control, signal conditioning and data processing. The micro-electronic fluidic (FlowFET) systems contain no moving part valves and are fully controllable by microelectronics [4]. The working principle is based on manipulating charges in a channel containing fluid by applying a perpendicular electric field on the channel wall. The main advantage of the FlowFET over the traditional mechanical pumps is that it has no moving parts thus easy to fabricate.

In previous studies, the electroosmotic flow was characterized for single channels as straight rectangular channel [5], channel with variable cross section like nozzle [6], or U-turn channel [7]. Also, very thin and therefore fragile micromachined silicon nitride tube structures were considered, having gate electrodes covered with thick silicon, which obstructed flow visualization in the gate region [4]. In the present study, the flow in a new configuration based on cross channels is analyzed, while the microfabrication process allows flow visualisation in the gate region.

2. Design and methods

The behavior-level simulation of a FlowFET provides the system designers with insights on how the change of system parameters, such as the gate voltage or the channel dimension, will affect the overall performance of the system [8]. Thus design decisions can be evaluated and optimization can be made. Recently, a new FlowFET has been designed [9]. The behavior of electroosmotic flow (EOF) in a straight channel has been modeled for operating conditions representing a fault-free case; the schematic layout of this structure is presented in figure 1.

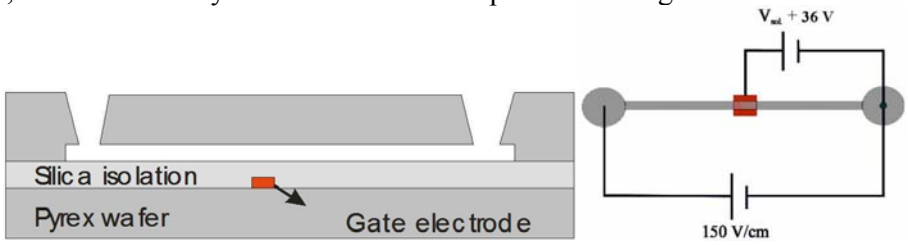

a) lateral view b) top view

Fig. 1 Schematic representation of the one channel structure

Based on these results, a new design was proposed to be simulated. The model describes the physical behavior of the fluid in a four channels array. This micro-electro-fluidic (MEF) array is composed of trapezoidal channels of the following dimensions: 18 μm deep, 70 μm top width and 30 μm bottom width. The platinum gate electrodes were separated from the microchannel by a 210 nm thick silicon oxide insulation layer. An electrical field of 150 V/cm was maintained along each of the intersecting channels while the gate potential was

varied between +36 V and −36 V relative to the potential in the channel. The system diagram is depicted in figure 2.

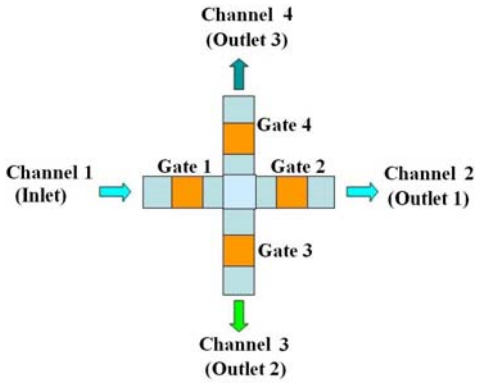

Fig. 2 Symbolic representation of the FlowFETs in a MEF array

The microchannel was filled with an aqueous buffer composed of a sodium acetate/acetic acid mixture having the following properties:

Table 1

Properties of aqueous buffer:

pH	4
Concentration	0.005 Moles
Dielectric constant	80
Viscosity	0.001 kg / m s
Conductivity	95 x 10^{-4} S/m

The electroosmotic flow is developed in the presence of ionized walls of microchannels and it is characterized by ζ-potential. This potential depends on the channels materials and charge of surfaces, which is influenced by Ph value of the buffer. When a voltage V_G is applied on the gate electrode (G), the ζ-potential has a different value ζ_G on the channel wall corresponding to the gate region, than on the other channel surfaces. The change in ζ-potential is given by:

$$\Delta\zeta = \frac{C_w}{C_d} V_G \tag{1}$$

where C_w is the capacitance of the channel wall and C_d is the capacitance of the electrical double layer. The capacitance (per unit area) of channel wall in the gate region is given by:

$$C_w = \frac{\varepsilon_r \varepsilon_0}{d} \tag{2}$$

where d is the thickness and ε_r is the dielectric constant of the oxide layer, while the capacitance (per unit area) of the electrical double layer can be estimated [4] as:

$$C_w = 2.285\sqrt{c}\cosh(19.46\zeta) \tag{3}$$

Equations (1) and (3) can be solved using a simple iterative technique to estimate the change in zeta potential under the gate electrode.

The electroosmotic effect can be modeled by a slip wall boundary condition:

$$v_{EO} = \mu_{EO}\vec{E} \tag{4}$$

where $\vec{E}$ is electrical field, μ is the coefficient of dynamic viscosity and μ_{EO} electroosmotic mobility given by:

$$\mu_{EO} = \frac{\varepsilon\varepsilon_0}{\mu} \tag{5}$$

In this way, the fluid flow can be controlled by the voltage applied on the gate electrode. The model was simulated using Coventorware software package, a dedicated tool to design and simulation of micro-electro-mechanical and microfluidic systems. The design module allows building the structures by 2D layout and deposition / etching steps similar to microfabrication technologies. The simulations were performed using NetFlow (Electrokinetic) module that can be applied to model coupled phenomena related to pressure driven flows and electrokinetic control.

At the inlet and outlet boundaries, the atmospheric condition in pressure have been considered, which is valid conditions for electroosmotic flow through long microchannels. First boundary condition in terms of voltage consists in 285 V between the source (S) and drain (D), equivalent to150 V/cm value for electric field along the channel. The voltage in the gate varies between [-36V … 36V]. The gate regions are assumed to be 175 μm long and are separated from the central channel intersection by a clearance of 3.5 μm.

3. Electroosmotic simulation results

The electroosmotic simulations considered four separate flow cases. To simplify the description of the various routing possibilities, the gate electrodes associated with the inlet, outlet 1, outlet 2 and outlet 3 channels are referred to as left, right, bottom and top respectively, as illustrated in figure 3.

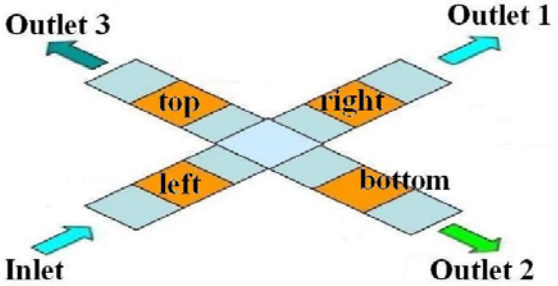

Fig. 3. Nomenclature of the gate electrodes for the electroosmotic simulations

Case 1 – The left and right gate electrodes are set to their maximum flow condition (Vg = −36 V; ζ = −42 mV) while the other two electrodes (top and bottom) are adjusted to obtain a no-flow condition through outlets 2 and 3:
- ζ-potential = -14 mV on non-gate regions
Left and right gates: ζ -potential = -42 mV
Top and bottom gate:
Case 1_1: ζ -potential = +21 mV
Case 1_2: ζ -potential = +5 mV
Case 1_3: ζ -potential = -14 mV
By linear interpolating, the value of ζ -potential for no flow was find:
Case 1_4: ζ -potential = 29.59 mV

In figure 4 the velocity distribution is presented in two longitudinal middle sections, along X and Y axis respectively, for case 1_4 (full flow in left-right direction and minimized flow in top and bottom channels). For a better view, the vectors length was 4 times exaggerated.

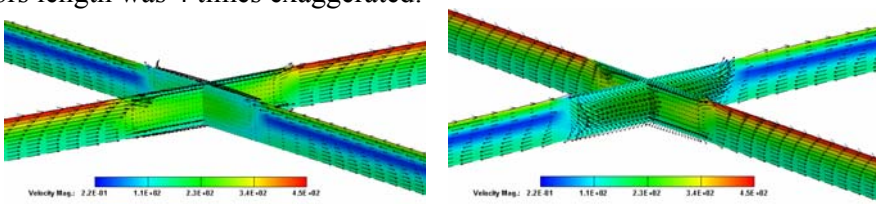

a) Normal (left-right) view b) Rotated view (270^0)

Fig. 4. Velocity distribution for case 1

The velocity is highest in active gate regions (left and right channels). The maximum velocity value tends to decrease and the vector changes its direction at short distance from the gates. There are two reasons for this variation. First, the change in ζ-potential at the end of the gate, from - 42 mV to -14 mV on top surface leads to decreasing of maximum value of velocity, while the mean value (defined as ratio between flow rate and area of cross section) remains constant in the channel since the flow is incompressible. Second, at the chamber inlet, the fluid flows from a smaller to a larger cross section area. In chamber region, not only the maximum velocity value is decreasing, but also the mean value. In the right channel, the velocity is increasing at short distance from the chamber under the right gate, and distribution becomes similar to the flow in left channel.

In top and bottom channels, the flow is influenced by the different values of ζ-potential. The main direction of flow is from top to bottom direction, corresponding to ζ = -14 mV. In the gate regions the flow is reversed as function of ζ-potential which has a different value and polarity: 29.59 mV. The mean velocity can be calculated by integrating the velocity over the cross area; since the direction is changing across this area, the mean velocity tends to zero and also the flow rate.

By post-processing the simulation results, it was found that the flow rate is not pure zero in top and bottom channels. This result could be the effect of non-zero ζ-potential in these channels. However, the order of magnitude is 10^{-5} nl, while in the left / bottom channels, the order of magnitude is 4 times higher: 0.1 nl.

Case 2: The top and right-hand gate electrodes are adjusted to obtain a no-flow condition through outlets 1 and 3, whilst the other two electrodes (left and bottom) are set to their maximum flow condition (Vg = −36 V; ζ = −42 mV). This results in the flow traveling through the MEF array from the inlet to outlet 2, with very little fluid lost to the top and right-hand channels. The conditions are:
ζ -potential = -14 mV on non-gate regions
- maximum flow from left channel to bottom channel: ζ -potential = -42 mV on left and bottom gate
- no flow in top / right channels: ζ -potential = 29.59 mV on top and right gate.
The velocity distribution is presented in figure 5.

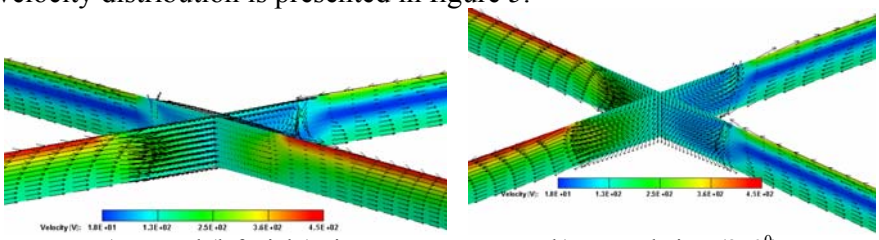

a) Normal (left-right) view b) Rotated view (270^0)

Fig. 5. Velocity distribution for case 2

The fluid is controlled to flow from left to bottom direction. The considerations discussed above are qualitatively the same. In the figures 4 a) and b) it can bee seen two views: the flow changes its direction and magnitude in the vicinity of chamber inlet. The maximum velocity values under the active gates – left and bottom channels are the same as in previous case. It can be seen that distribution is non-symmetric: in the left channel – chamber inlet region, the velocity tends to change orientation not only in Z-direction but also in Y direction (to bottom), and in the bottom channel – chamber outlet region, the velocity tends to change orientation also in X direction (to right).

Case 3: Similar to case 1 but with an assumed surface treatment along the non-gated regions so that the zeta potential at the wall is zero. The gate voltages on the top and bottom electrodes are adjusted to give ζ = 0 in order to obtain the no-flow condition though outlets 2 and 3:
Left and right gates regions: ζ-potential = -42 mV
Top and bottom gate and non-gate regions: ζ-potential = 0
Figure 6 shows the velocity distribution for this case

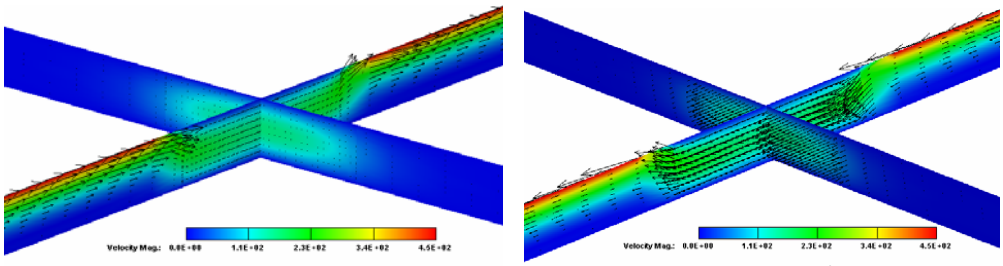

a) Normal (left-right) view b) Rotated view (270^0)

Fig. 6. Velocity distribution for case 3

The active regions are only left and right gates with ζ-potential = -42 mV. Top and bottom gate and non-gate regions are tread as ζ-potential = 0. The figures 3 a) and 4 illustrate two views. By comparison to case 1, the flow profile shows the same maximum values in left and right channels under the gate regions, but is zero in the vicinity of non gated surfaces. In top and bottom channel, flow profile is essentially different. Except the chamber region having velocity of ~ 250 μm / s, the velocity in top and bottom channels is zero. That means that in all regions where ζ-potential is zero, there is no flow since electroosmotic mobility is also zero.

Case 4 is similar to case 2 but again with an assumed surface treatment along the non-gated regions so that the zeta potential at the wall is zero. The gate voltages on the top and right-hand electrodes are adjusted to give ζ = 0 in order to obtain the no-flow condition though outlets 1 and 3. The other two gate electrodes (left and bottom) are set to their maximum flow condition (Vg = −36 V; ζ = −42 mV). The velocity distribution is presented in figure 7.

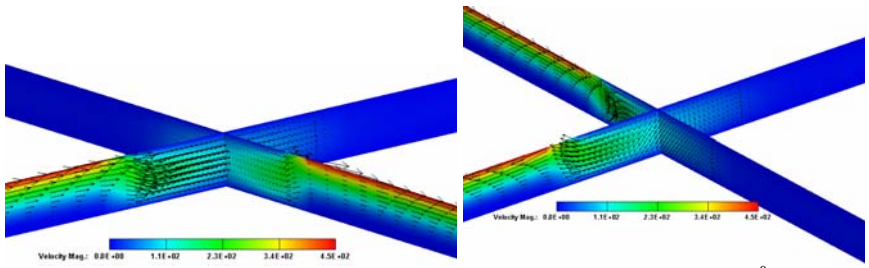

a) Normal (left-right) view b) Rotated view (270^0)

Fig. 7. Velocity distribution for case 4

In the region between left gate and chamber inlet, flow direction change in negative Z-direction (fluid flows towards the bottom surface) and in negative Y-direction (fluid flows towards the bottom channel). In the region between chamber outlet and bottom gate, flow direction change in positive Z direction

(fluid flows towards to the top surface) and in positive X direction. The non-symmetry (as function of Y axis) of flow in bottom channel at the entrance in gate region can be related to inertial forces of flow when the fluid pass the chamber and change from X to Y direction.

4. FlowFET Driven EOF Measurements

To measure the quantitative and qualitative influence of a heterogeneous zeta potential on the velocity profile and flow rate, Particle Image Velocimetry (PIV) has been used. In PIV, tracer particles are added to the solution inside the channel. Subsequently, two images are taken with a short time interval. After this, the displacement of the beats in sub-windows of the frames are determined and divided by the time interval to get the velocity vectors. The displacement of the tracer particles inside a sub-window of a frame is determined by the Minimum Quadratic Difference (MQD) algorithm. With this algorithm the quadratic difference in pixel intensity is evaluated when one sub-window is displaced with respect to the second one. The velocity vector for the sub-window is calculated with the displacement of the first sub-window where a minimum in quadratic difference in pixel intensity is determined. Figure 8 give an example of a velocity profile with and without a gate potential.

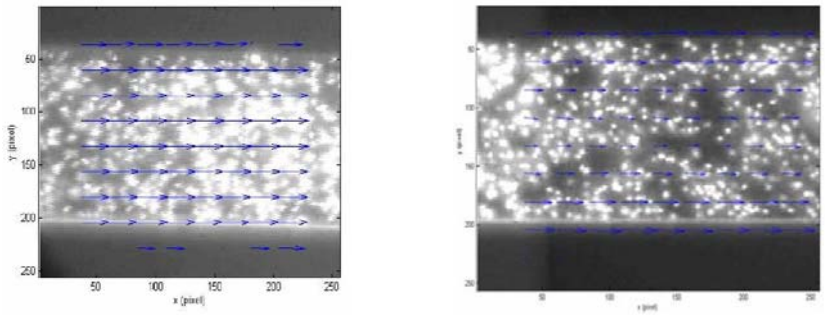

a) Velocity profile without gate potential b) Velocity profile with positive gate potential

Fig. 8. Velocity distribution (Time interval between cross correlated images is 40 micro seconds.)

The vectors indicate the velocity. Figure 8a shows a uniform velocity profile over the cross section of the channel. When a positive gate potential is applied, the velocity shows a concave profile with a minimum in the center of the channel. This is caused by the influence of the gate potential. The positive gate potential leads to a more positive zeta potential in the gate region and thus a difference in EOF in the gate and non-gate region. This difference in EOF induces a pressure driven flow in the direction opposite to the EOF. The velocity profile than consists of an EOF and a hydrodynamic component as can be seen in figure 8b.

5. Conclusions

The scope of this work was to investigate the electro osmotic in cross channels and to find the appropriate parameters to control the flow in the channels. The flow direction can be controlled by ζ-potential applied on active gates. The major findings can be summarized as follows:
(1) The flow simulations for an unmodified zeta potential of −14 mV along the non-gated regions of the MEF array demonstrate that fluidic routing between the inlet channel and the various outlet channels is feasible by carefully controlling the zeta potential along the "blocked" channels.
(2) By comparison of the two set of results for non-flow conditions in blocked channels, it was shown that the control is much efficient in case of zero ζ-potential on channels walls and non-active gates: the velocity in these regions is zero, and, consequently, the flow rate is zero. In case of ζ-potential = - 14 mV on the channels walls and interpolated value ζ-potential = 29.59 mV on the gates, the flow presents large recirculating eddies in the blocked channels which may produce undesired mixing between the various channels within the array.
(3) The flow simulations for a modified MEF array (where the non-gated wall regions are assumed to have undergone a surface treatment) show that the recirculating eddies can be completely eliminated if the zeta potential is reduced to zero. In addition, the fluidic routing at the intersection appears to be more uniform in the modified design.
(4) An additional advantage of adopting the modified design is that the zeta potential required to achieve the blocking effect does not have to be determined by special calibration of the device. This would considerably simplify the operating conditions of the MEF array.

The application area of this type of array is expected to be significantly larger (e.g. automatic chemical & drug synthesis) and of clear industrial interest. The main advantages of these systems are the array configuration of channels that allow swiching operation, and also speed of operation, use of very small amounts of liquid, on-board detection, and their suitability for mass fabrication. Another significant advantage is given by the integrated electronic part that ensure a high level of automation [10,11].

Acknowledgements

This research was performed in the frame of FP 6 European project "Design for Micro and Nano Manufacture – PATENT DfMM" Network of Excellence, WP2 Modelling and Simulation, Research Grant "Fault Modelling and System Simulation of FlowFET MEF Arrays".

REFERENCES

[1]. *N. T. Nguyen and S. T. Wereley*, Fundamentals and Applications of Microfluidics, Artech House Inc., 2002.
[2]. *D. Li*, Electrokinetics in Microfluidics, Elsevier, 2004
[3]. *T. Zang, K. Chakrabaty, R. Fair*, "Microelectrofluidic Systems: Modelling and Simulation", CRC Press, Boca Raton USA, 2002
[4]. *R.B.M. Schasfoort, S. Schlautmann, J. Hendrikse, A. van den Berg* "Field-Effect Flow Control for Microfabricated Fluidic Networks", Science, **Vol. 286**, October 1999, pp. 942-945
[5]. *Sadr, R., Yoda, M., Zheng, Z., Conlisk, A. T.*An experimental study of electro-osmotic flow in rectangular microchannels, Journal of Fluid Mechanics, 506, 357-367, 2004
[6]. *Chen, Lei, Conlisk, A. T.,* Electroosmotic flow and particle transport in micro/nano nozzles and diffusers, Biomedical Microdevices, 10, Issue: 2, 289 - 298, 2008
[7]. *Gea O. F. Parikesit, Anton P. Markesteijn, Vladimir G. Kutchoukov, Oana Piciu, Andre Bossche, Jerry Westerweel, Yuval Garini, Ian T. Young*, Electroosmotic flow analysis of a branched U-turn nanofluidic device, Lab Chip Journal, 2005, 5, 1067–1074
[8]. *H.G. Kerkhoff, R.W. Barber, D.R. Emerson, R. Muller, O.T. Nedelcu, E. van der Wouden,* "Design and Test of Micro-Electronic Fluidic Systems", Workshop on MEMS, Design, Automation and Test in Europe Conference, 7-11 March 2005, Munich, Germany
[9]. *O. T. Nedelcu, R. W. Barber, H. G. Kerkhoff, D. R. Emerson, R. Muller, E. Van Der Wouden,* "Modelling of Micro-Electronic Fluidic Systems", Romanian Journal of Information Science and Technology, **Vol. 8**, No. 4, 2005, pp. 363-370
[10] *Andrei Drumea, Paul Svasta,* Microcontroller-based electronic module for controlling mechatronic systems, UPB Sci. Bull. Series C, **Vol.71**, Iss.2, 2009
[11] *Dan Olaru, Dan Floricău,* Optimal method for controlled switching circuits, UPB Sci. Bull. Series C, **Vol.71**, Iss.3, 2009.